

The bulge-halo conspiracy in massive elliptical galaxies: implications for the stellar initial mass function and halo response to baryonic processes

Aaron A. Dutton^{1*} & Tommaso Treu²

¹*Max Planck Institute for Astronomy, Königstuhl 17, D-69117 Heidelberg, Germany*

²*Department of Physics, University of California, Santa Barbara, CA 93106, USA*

submitted to MNRAS

ABSTRACT

Recent studies have shown that massive elliptical galaxies have total mass density profiles within an effective radius that can be approximated as $\rho_{\text{tot}} \propto r^{-\gamma'}$, with mean slope $\langle \gamma' \rangle = 2.08 \pm 0.03$ and scatter $\sigma_{\gamma'} = 0.16 \pm 0.02$. The small scatter of the slope (known as the bulge-halo conspiracy) is not generic in Λ cold dark matter (Λ CDM) based models and therefore contains information about the galaxy formation process. We compute the distribution of γ' for Λ CDM-based models that reproduce the observed correlations between stellar mass, velocity dispersion, and effective radius of early-type galaxies in the Sloan Digital Sky Survey. The models have a range of stellar initial mass functions (IMFs) and dark halo responses to galaxy formation. The observed distribution of γ' is well reproduced by a model with cosmologically motivated but uncontracted dark matter haloes, and a Salpeter-type IMF. Other models are on average ruled out by the data, even though they may happen in individual cases. Models with adiabatic halo contraction (and lighter IMFs) predict too small values of γ' . Models with halo expansion, or mass-follows-light predict too high values of γ' . Our study shows that the non-homologous structure of massive early-type galaxies can be precisely reproduced by Λ CDM models if the IMF is not universal and if mechanisms such as feedback from active galactic nuclei, or dynamical friction, effectively on average counterbalance the contraction of the halo expected as a result of baryonic cooling.

Key words: stars: luminosity function, mass function – galaxies: elliptical and lenticular, cD – galaxies: formation – galaxies: fundamental parameters – dark matter

1 INTRODUCTION

Recent observations combining stellar kinematics with strong gravitational lensing from the Sloan ACS lens Survey (SLACS; Bolton et al. 2006, 2008; Auger et al. 2009) have shown the total mass density profiles of massive elliptical galaxies (i.e. with stellar mass above $M_{\text{star}} \sim 10^{11} M_{\odot}$ or stellar velocity dispersion $\sigma > 200 \text{ km s}^{-1}$) are very close to isothermal (Treu & Koopmans 2004; Koopmans et al. 2006, 2009; Auger et al. 2010b; see also, e.g., Bertin et al. 1994, Franx et al. 1994, Dobke & King 2006, Gavazzi et al. 2007, Humphrey & Buote 2010 for additional probes pointing in the same direction). The high precision lensing and dynamical measurements show that within the effective or half-light radius, the average logarithmic slope of the mass density

profile ($\rho_{\text{tot}} \propto r^{-\gamma'}$) is $\langle \gamma' \rangle = 2.078 \pm 0.027$ with an intrinsic scatter of $\sigma_{\gamma'} = 0.16 \pm 0.02$ (Auger et al. 2010b).

The physical origin of this observational result is at present not fully understood. We first note that the mass density profiles of stars and Λ cold dark matter (Λ CDM) haloes are different from isothermal near the effective radius: If mass-follows-light (MFL), then for a de Vaucouleurs profile $\gamma' \sim 2.3$. In contrast, if dark matter dominates, then $\gamma' \lesssim 1.5$. The observational fact that $\gamma' \simeq 2$ implies that both baryons and dark matter contribute non-negligible fractions to the mass within the effective radii of massive ellipticals. This is sometimes referred to as the “bulge-halo conspiracy” – the baryons and dark matter must “know” about each other so that the total mass profile that results from summing the two non-isothermal components is close to isothermal. In other words the observation can be qualitatively reproduced by combining standard Λ CDM haloes

* dutton@mpia.de

with stellar mass density profiles, but only with appropriate fine tuning of the stellar to dark matter ratio, or equivalently of the star formation efficiency (e.g. Keeton 2001; Gavazzi et al. 2007; Jiang & Kochanek 2007; Auger et al. 2010a; Nipoti, Treu & Bolton 2008).

Remarkably, the bulge-halo conspiracy does not happen at all scales. For example, the total mass density profile of galaxy clusters with a massive galaxy at the centre is known to be inconsistent with isothermal (e.g., Allen et al. 2008; Newman et al. 2013a,b). Since dark matter haloes are almost scale invariant in Λ CDM (except for mild trends in concentration, e.g. Macciò et al. 2008), this difference suggests that understanding the origin of the bulge-halo conspiracy requires understanding the relevant baryonic physics. Attention has therefore turned to cosmological hydrodynamical simulations of galaxy formation.

Duffy et al. (2010) found that simulations with no or weak feedback can reproduce the observed γ' , but they overpredict the galaxy formation efficiencies (see also Naab et al. 2007). Strong feedback is needed to match the observed baryon fractions, but the resulting galaxies have γ' that is too small (i.e. the galaxies are dark matter dominated). The simulations used by Duffy et al. (2010) were stopped at $z = 2$, so their conclusions are only valid if γ' does not evolve. Johansson et al. (2012) ran nine high resolution “zoom-in” simulations of $\sim 10^{12} M_{\odot}$ dark matter haloes down to $z = 0$ (see also Remus et al. 2013). These simulations have γ' in good agreement with observations at $z \sim 0$, and also find γ' evolves from $\gamma' \sim 3$ at high redshifts to $\gamma' \sim 2$ below $z \sim 1$. However, these simulations (which do not have strong feedback) overpredict the galaxy formation efficiencies by a factor of $\sim 2-3$, even assuming a Salpeter (1955) stellar initial mass function (IMF). More recently Dubois et al. (2013) simulated six haloes in the mass range $0.4 - 8 \times 10^{13} M_{\odot}$ both with and without feedback from active galactic nuclei (AGN). At $z = 0$ the simulations without AGN feedback resulted in too many baryons and overpredict the mass density slopes ($\gamma' \sim 2.3$), while the simulations with AGN feedback reproduce the galaxy formation efficiencies (assuming heavy IMFs in more massive galaxies), but under predict the mass density slopes ($\gamma' \sim 1.9$). *Thus at present, none of the cosmological simulations in the literature can simultaneously match the observed γ' and galaxy formation efficiencies at $z \sim 0$.*

In this paper we aim to shed light on this issue by performing a quantitative comparison of flexible Λ CDM - inspired models to the observed distribution of γ' in lens galaxies. First, we investigate how dark matter fraction is required in order for models to reproduce the observed distribution of γ' . If a model has the right (i.e., observed) amount (and distribution) of baryons) are the theoretical properties of Λ CDM haloes sufficient to explain the observed properties of γ' ? A second question we address is to what extent γ' can help to constrain the dark matter fractions inside an effective radius, and hence to constrain the stellar IMF and dark halo response to galaxy formation.

Observationally, a common way of measuring the dark matter fraction within an effective radius is achieved by “subtracting” the stellar mass from the total mass. Total masses are relatively straight forward to measure (either through dynamics and/or strong lensing), but stellar masses from spectral energy distributions are uncertain by a fac-

tor of ~ 3 due to the unknown form of the IMF (e.g. Bell et al. 2003).

Star counts in stellar clusters are consistent with a universal IMF *within the Milky Way* (e.g., Bastian, Cover, Meyer 2010). Dynamical mass-to-light ratios of extragalactic spiral galaxies are also consistent with a Milky Way IMF (e.g., Bell & de Jong 2001), and inconsistent with the heavier¹ Salpeter (1955) IMF. Dynamical mass-to-light ratios of galaxies in the SAURON survey argue against a universal Salpeter IMF in early-type galaxies (Cappellari et al. 2006; Tortora et al. 2012), but they do not rule out a Salpeter-type IMF in all early-type galaxies. In fact, Salpeter-type IMFs are preferred in massive elliptical galaxies, even accounting for standard dark matter haloes (Treu et al. 2010; Dutton et al. 2011). Furthermore, there are several lines of evidence that *require* massive elliptical galaxies and even massive spiral bulges to have IMFs significantly heavier than that found in the Milky Way (e.g., Auger et al. 2010a; van Dokkum & Conroy 2010; Conroy & van Dokkum 2012; Cappellari et al. 2013; Dutton et al. 2013a,b).

Theoretically, the dark matter fraction within the effective radius depends on the efficiency of galaxy formation, the structure of “pristine” dark matter haloes, and the response of the dark matter halo to galaxy formation. Galaxy formation efficiencies are hard to predict theoretically, but can be constrained through observations of weak lensing and satellite kinematics (e.g., Mandelbaum et al. 2006; More et al. 2011). In the framework of Λ CDM the pristine structure of dark matter haloes is known (for a given set of cosmological parameters), but the response of the dark matter halo is not well constrained by theory. Gas cooling or gas rich (dissipational) mergers are expected to make the dark halo contract (Blumenthal et al. 1986; Gnedin et al. 2004). Mass outflows (feedback) or gas poor (dissipationless) mergers are expected to make the dark halo expand (e.g., Read & Gilmore 2005; Governato et al. 2010; Pontzen & Governato 2012; Macciò et al. 2012; El-Zant et al. 2001; Nipoti et al. 2004; Jardel & Sellwood 2009; Johansson et al. 2009; Teyssier et al. 2011). The relative importance of each of these processes will determine the response of the dark matter halo to galaxy formation.

In practice, we address the two questions by using Λ CDM based models (from Dutton et al. 2013b) that are constructed to reproduce a number of scaling relations of early-type galaxies including: velocity dispersion versus stellar mass; half-light size versus stellar mass and dark halo mass versus stellar mass. The main unknowns in these models are the normalization of the stellar mass (and therefore the stellar IMF) and the response of the dark matter halo to galaxy formation.

This paper is organized as follows: our definition of γ' is given in §2. The constrained galaxy mass models are briefly discussed in §3. Results are presented in §4. The method used to measure ensemble average mass density slopes is discussed in §5. A brief discussion is given in §6, followed

¹ By heavier we mean that the IMF results in higher stellar mass-to-light ratios in old stellar populations. This could result from either an excess of low-mass stars (from a bottom heavy IMF), or from an excess of stellar remnants (from a top heavy IMF)

by conclusions in §7. We adopt a Λ CDM cosmology with $\Omega_\Lambda = 0.7$, $\Omega_M = 0.3$ and $H_0 = 70 \text{ km s}^{-1} \text{ Mpc}^{-1}$

2 DEFINITION OF MASS DENSITY SLOPE

There are many different definitions for the mass density slope of galaxies used in the literature. We have chosen our definition primarily to enable a meaningful comparison to the mass density slopes derived from joint strong lensing and dynamics analyses (e.g., Koopmans et al. 2009). In addition, our definition is simple to compute and can be applied to all type of galaxies (spirals as well as ellipticals).

We adopt the mass weighted slope within the effective radius (which, we show below is equivalent to the mass slope at the effective radius) as heuristically strong lensing and stellar dynamics measure the total *mass* (rather than density) within different radii. These radii are typically close to the effective radius, hence a joint strong lensing and dynamics analysis measures the slope of the total mass profile near the effective radius.

For an arbitrary density profile, $\rho(r) \propto r^{-\gamma(r)}$, the local logarithmic slope of the density profile is $d \log \rho / d \log r \equiv -\gamma(r)$. We follow the convention of Koopmans et al. (2009) that $\gamma > 0$. Thus the mass weighted slope of the density profile within radius r is given by

$$\gamma'(r) = \frac{1}{M(r)} \int_0^r -\gamma(x) 4\pi x^2 \rho(x) dx = 3 - \frac{4\pi r^3 \rho(r)}{M(r)}. \quad (1)$$

This can be expressed in terms of the local logarithmic slopes of the mass, $M(r)$, and circular velocity, $V(r)$ profiles:

$$\gamma'(r) = 3 - \frac{d \log M}{d \log r} = 2 - 2 \frac{d \log V}{d \log r}. \quad (2)$$

In the case of a power-law density profile $\gamma'(r) = \gamma$. But in general, i.e., for a non power-law density profile, $\gamma'(r) \neq \gamma(r)$. Since galaxies have mass density profiles with slopes that decrease (i.e., become more negative) with increasing radius, the mass weighted slope is less than the local slope: $\gamma'(r) < \gamma(r)$. For example, for an NFW profile (which has an inner density slope of -1 and outer slope of -3) at the scale radius $\gamma(r_s) = 2$ whereas $\gamma'(r_s) \simeq 1.7$, and for a Hernquist profile (inner slope -1 , outer slope -4) at the effective radius $\gamma(R_e) \simeq 2.9$ whereas $\gamma'(R_e) \simeq 2.3$. In the following we will use the shorthand notation γ' and to indicate the mass weighted average slope within the effective radius.

3 MASS MODELS OF EARLY-TYPE GALAXIES WITH Λ CDM HALOES.

This section gives a brief overview of the mass models we construct to reproduce the observed structural and dynamical scaling relations of early-type galaxies in the Sloan Digital Sky Survey (SDSS; York et al. 2000; Abazajian et al. 2009). A more detailed discussion is given by Dutton et al. (2013b). Our mass models consist of spherical distributions of stars and dark matter. The stars are modelled as the sum of two Sérsic profiles (with $n = 1$ and $n = 4$), while the dark matter is an NFW (Navarro, Frenk, & White 1997) profile with “pristine” concentration parameters from Macciò et al. (2008) and modified by halo contraction/expansion following Dutton et al. (2007).

High resolution cosmological simulations have shown that at small radii ($\sim 1\%$ of the virial radius) dark matter haloes have steeper density profiles than the NFW formula. A number of studies have shown that the Einasto (1965) profile ($d \ln \rho / d \ln r \propto r^\alpha$), provides, in general, a better description of CDM haloes than the NFW profile (e.g., Navarro et al. 2004, 2010; Merritt et al. 2005, 2006; Stadel et al. 2009; Reed et al. 2011). Reed et al. (2011) show that the variation in density profiles of massive dark matter haloes are fully explained by an Einasto profile with $\alpha = 0.19$ together with the usual scatter in the halo concentration parameter. To determine whether our results are sensitive to the difference between NFW and Einasto haloes at small radii we have re-computed our uncontracted models using the Einasto profile, and kept all other parameters the same as in the original NFW model. The increased dark matter density at small radii from the Einasto profile results in just a 1% increase in aperture velocity dispersion, 2% decrease in mass density slope (γ') and a 6% increase in the scatter in γ' . Thus in what follows we predominantly focus on results with NFW haloes.

The stellar profiles of the models are constructed to reproduce the size-mass relation of early-type galaxies from Dutton et al. (2013b) which uses sizes from Simard et al. (2011), and stellar masses from the MPA/JHU group² which assume a Chabrier (2003) IMF. The halo masses are chosen to follow the observed relation between stellar mass and halo mass for early-type galaxies from Dutton et al. (2010) which combines results from weak lensing (e.g., Schulz et al. 2010) and satellite kinematics (e.g., More et al. 2011). The models have three sources of scatter: scatter in galaxy size at fixed stellar mass (constrained by observations: Dutton et al. 2013b); scatter in dark halo mass at fixed stellar mass (constrained by observations: More et al. 2011); and scatter in dark halo concentration at fixed dark halo mass (constrained by theory: Macciò et al. 2008).

The velocity dispersion versus stellar mass (a.k.a. Faber & Jackson 1976) relation is used to constrain the allowed combinations of stellar IMF and dark halo response in these models. We consider five different halo responses ranging from standard adiabatic contraction (Blumenthal et al. 1986) to unmodified NFW haloes to MFL (i.e., maximum expansion). In order to reproduce the slope and zero-point of Faber-Jackson relation, all these models require “heavier” IMFs in more massive galaxies, and (trivially) “heavier” IMFs in models with stronger halo expansion. These set of models are physically realistic (at least in terms of reproducing the scaling relations) while having a wide range of dark matter fractions and inner dark matter halo density profiles.

The correlation between the scatter in the velocity-mass relation with the scatter on the size-mass relation – equivalent to the tilt of the Fundamental Plane (FP; Dressler et al. 1987; Djorgovski & Davis 1987; Ciotti et al. 1996) – was used by Dutton et al. (2013b) as an additional constraint to distinguish between these models. For galaxies in the mass range $10^{10} \lesssim M_{\text{SPS}} \lesssim 10^{11} M_\odot$, only models in which MFL were able to match this additional constraint. For the most massive galaxies (and those which are relevant

² Available at <http://www.mpa-garching.mpg.de/SDSS/DR7/>

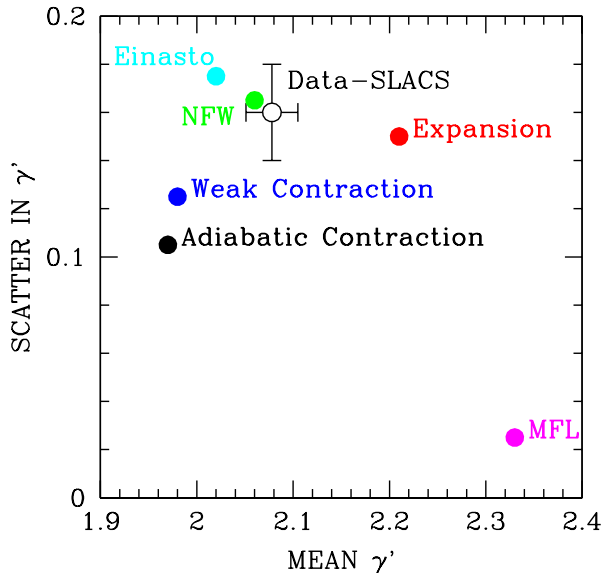


Figure 1. Mean and scatter of the mass weighted density slope within an effective radius, γ' , for models (from Dutton et al. 2013b) and data (from SLACS – Auger et al. 2010b). The mean and scatter of γ' are only jointly reproduced in our model with uncontracted cosmologically motivated NFW haloes and a heavy Salpeter-type IMF (green point). Models with expansion (red point) or mass follows light (MFL - magenta point) overpredict the mean γ' , while models with halo contraction (blue and black) under predict both the mean and scatter. A model with unmodified Einasto dark matter haloes (cyan point) yields similar results as the NFW model.

for this paper), models with unmodified NFW haloes were favoured over MFL and adiabatic contraction models.

4 RESULTS

In order to make a fairer comparison between our models and data from SLACS we consider model galaxies that match the distribution of velocity dispersions for the SLACS lenses. Specifically, we select model galaxies with a log-normal filter on velocity dispersion: $\text{mean}(\log(\sigma/[\text{km s}^{-1}])) = 2.40$ and standard deviation 0.07. With this selection the average offset between the model stellar masses and those obtained assuming a Chabrier IMF are $\Delta_{\text{IMF}} = \log_{10}(M_{\text{star}}/M_{\text{SPS}}) = (0.08, 0.20, 0.27, 0.31, 0.33)$ for halo responses of $\nu = (1.0, 0.5, 0.0, -0.5, \text{MFL})$, respectively³. For reference, a Salpeter IMF corresponds to $\Delta_{\text{IMF}} \simeq 0.23$, and thus, models with uncontracted dark matter haloes ($\nu = 0.0$) and expansion ($\nu = -0.5$) have IMFs heavier than Salpeter.

The observed γ' are not strictly measured within any uniform aperture such as one effective radius, R_e . The aperture depends on the Einstein radius and the physical aperture of the SDSS fibre. The former depends on the velocity dispersion of the lens and the redshifts of the lens and source,

³ For easy comparison with previous studies $\Delta_{\text{IMF}} = \log \alpha$, where α is the so-called IMF mismatch parameter, e.g., Treu et al. (2010), Dutton et al. (2013a).

while the latter just depends on the redshift of the lens. However, for SLACS lenses the aperture is typically between one and one-half an effective radii (e.g., Koopmans et al. 2009). To test whether γ' depends on the radius within which it is measured we have compared γ' within R_e and $R_e/2$. In general $\gamma'(R_e/2) < \gamma'(R_e)$, but the changes are small. The changes in the median γ' for our five models are as follows: $\gamma'(R_e) - \gamma'(R_e/2) = (0.028, 0.022, 0.001, 0.070, 0.141)$ for halo responses of $\nu = (1.0, 0.5, 0.0, -0.5, \text{MFL})$. Thus, the mass density slopes varies between one and one-half an effective radius by much less than the intrinsic scatter, except for the MFL model, which we will show below is a poor match to the data for other reasons (and is well known to be a poor match to massive elliptical galaxies anyway). For simplicity, in what follows we measure the mass density slopes within one effective radius, with no significant loss of precision.

Our main results are summarized in Fig. 1, which shows the scatter in γ' versus the mean of γ' for our five models and observations from Auger et al. (2010b). The distributions of γ' for the four models with dark matter haloes are shown in Fig. 2. The model with MFL is only comprised of stars and therefore has $\gamma' = 2.33^{+0.02}_{-0.03}$.

4.1 Average mass density slopes

All of the models broadly reproduce the close to isothermal density profiles that are observed, with average slopes in the range $1.8 \lesssim \gamma' \lesssim 2.4$. However the model with uncontracted NFW haloes (and a slightly heavier than Salpeter IMF) provides the best match to the observed average γ' (Fig. 1 and yellow shaded region in Fig. 2). This is in good agreement with the conclusions of Auger et al. (2010a) who favoured uncontracted haloes over any type of halo contraction (they did not consider expansion or MFL), and IMFs significantly heavier than Chabrier. It is also in excellent agreement with the, *completely independent*, constraints from the tilt of the fundamental plane from Dutton et al. (2013b).

4.2 Scatter in mass density slopes

Most importantly however, our models also reproduce the observed scatter of the distribution, i.e. the tightness of the bulge-halo conspiracy. The distribution of γ' in the models is roughly Gaussian (although slightly skewed) with scatter smaller or equal to the observed intrinsic scatter of 0.16 ± 0.02 . As with the mean γ' , the model with uncontracted NFW haloes best matches the scatter with $\gamma' = 2.06^{+0.14}_{-0.19}$.

Given that there is significant overlap between the observed distribution of γ' and all of our models, it is entirely possible that the full range of halo responses occurs in real galaxies. Indeed, there are already observational hints that this is the case. While on average a Salpeter-type IMF favours uncontracted NFW haloes (e.g., Treu et al. 2010; Auger et al. 2010a; Dutton et al. 2011, 2013b), the detailed study of a massive elliptical, enabled by the presence of a double Einstein Ring, favours a Salpeter-type IMF and a contracted halo (Sonnenfeld et al. 2012). From a theoretical standpoint, this could be connected to the specific merger history of each galaxy (e.g., Nipoti et al. 2012 and references therein) or perhaps to the mode of star formation and resulting IMF (Hopkins 2013). Below, we will explore whether

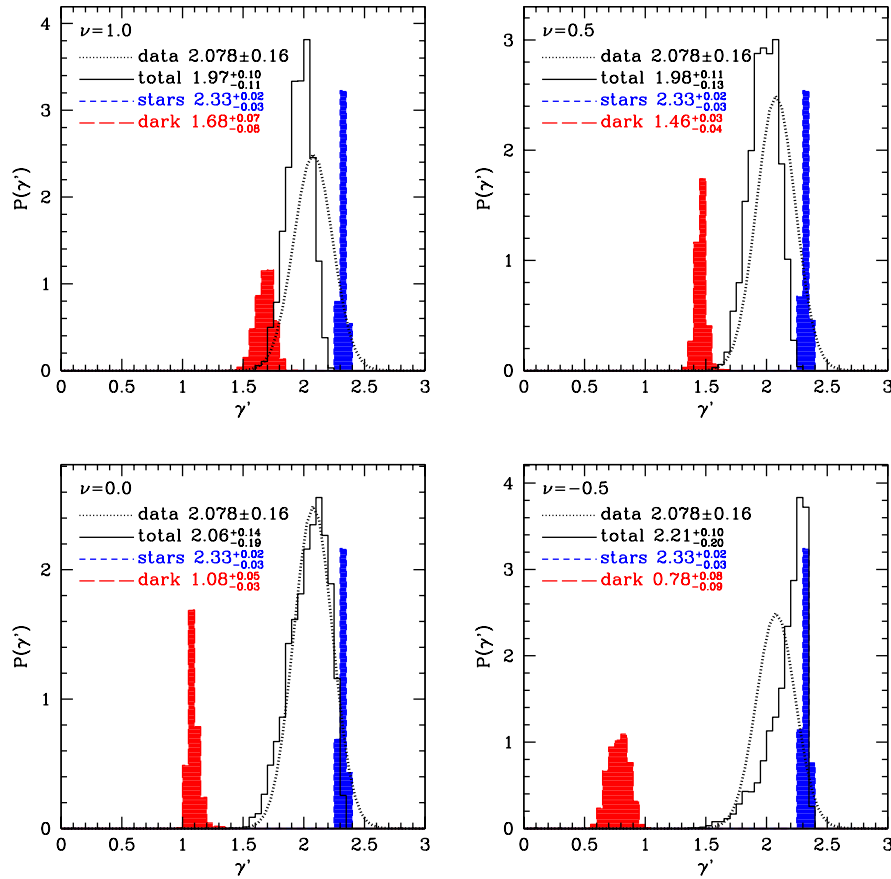


Figure 2. Distribution of mass-weighted density slope within an effective radius, γ' , for our models compared with the observed (intrinsic distribution) from Auger et al. (2010b, black dotted line). The histograms show γ' for the total mass (black, solid), stellar mass (blue, short dashed), and dark matter (red, long dashed). Each panel has a model with a different dark halo response: adiabatic contraction, $\nu = 1.0$ (upper left); mild contraction $\nu = 0.5$ (upper right); no contraction $\nu = 0.0$ (lower left); and expansion $\nu = -0.5$ (lower right). The model with mass-follows-light is equivalent to that of the stellar component. Only the model with uncontracted cosmologically motivated dark matter haloes and a heavy IMF reproduces the observations.

γ' correlates with other observables. This could potentially provide some clues as to the origin of each galaxy.

4.3 Mass density slopes of stars and dark matter

In Fig. 2, the red histograms show the mass-weighted density slopes within R_e of the dark matter haloes, γ'_{DM} . These range from $\simeq 1.7$ for adiabatic contraction, to $\simeq 0.8$ for expanded haloes. The blue histogram shows the mass-weighted density slopes within R_e of the stars, these have $\gamma'_{\text{star}} \simeq 2.33 \pm 0.02$.

The relative contribution of the stars and dark matter to the total γ' is given by the dark matter fraction within an effective radius, $f_{\text{DM}}(R_e)$. As expected, for a given halo response model γ' is strongly anti-correlated with the dark matter fraction (Fig. 3). The lines show the median γ' as a function of dark matter fraction, while the dots show the median γ' and $f_{\text{DM}}(R_e)$. While for an arbitrary halo response γ' does not uniquely predict the dark matter fraction, it does place some useful limits. For example, if $\gamma' > 2$, then $f_{\text{DM}}(R_e) < 0.2$.

The average dark matter fractions vary from $\simeq 0.55$ for

adiabatic contracted NFW haloes (black dot) to $\simeq 0.10$ for expanded NFW haloes (red dot). For NFW haloes (green dot), the average dark matter fraction is just $\simeq 20\%$, but this is enough to lower the mean γ' by 0.27 and increase the scatter in γ' by 0.14 relative to the MFL model.

Note that in our model the variation in dark matter fraction within the effective radius is driven by all three sources of scatter: the global stellar to virial mass ratio; the concentration parameter of the halo; and the effective radius of the galaxy. The former two result in scatter in the dark matter mass within fixed radius, while the latter changes the physical radius where the dark matter fraction is measured (as well as changing the dark matter mass through the differential halo response).

4.4 What does γ' correlate with?

Previous observational studies have shown that γ' is largely uncorrelated with many physical properties of galaxies, and does not evolve significantly since $z \sim 1$ (e.g., Koopmans et al. 2009; Auger et al. 2010b; see however Ruff et al. 2011 and Bolton et al. 2012 for tentative detections of a mild

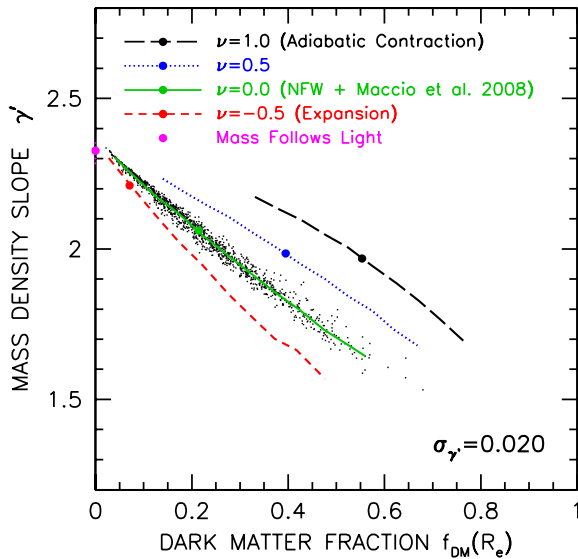


Figure 3. Correlation between mass density slope, γ' , and dark matter fraction within an effective radius, f_{DM} , for our models. The coloured lines show the median mass density slope as a function of the (spherical) dark matter fraction, while the dots show the median values. For a given halo response the mass density slope is determined by the dark matter fraction.

evolutionary trend). The most significant correlation found by Auger et al. (2010b) was between γ' and total surface density, with denser galaxies having higher γ' . Such a correlation is expected because denser galaxies have either higher density stellar components (which increases the contribution of the stars to γ') and/or stronger halo contraction (which results in higher γ'_{DM}). This correlation might provide an important clue to understanding the origin of the small variations from galaxy to galaxy. The central density could be a by-product of the epoch of formation of the initial core and successive merger history and perhaps be related to the conditions of the gas that created the bulk of the old stars.

Fig. 4 shows correlations between γ' and a number of physical galaxy parameters: stellar surface mass density; effective radius; stellar mass; and stellar velocity dispersion. Lines show the median relations for the models, the points show the model galaxies with uncontracted NFW haloes, and the filled points with error bars show the observations from SLACS (Auger et al. 2010b). To ease comparisons between the different models and the data the stellar masses and stellar densities have been re-scaled to a Salpeter IMF. The most significant correlation in the data is with stellar density, followed by effective radius and stellar mass. These trends are qualitatively reproduced by the models. To the eye, the data appear to suggest a weak positive correlation with velocity dispersion, which is of opposite sign to the models. However, the measurement errors on γ' are positively correlated with the errors on σ_{e2} (Auger et al. 2010b), and therefore the trend is statistically insignificant (slope 0.07 ± 0.08) and consistent with the weak opposite trend seen in our models.

Thus, not only does our model with uncontracted NFW haloes reproduce the mean and scatter of the observed γ' , it

also reproduces the correlations between γ' and other galaxy observables. We note this achieved without any arbitrary fine-tuning of the distribution of baryons and dark matter in galaxies.

In our models, for a given halo response, there is almost no scatter between γ' and dark matter fraction. Thus the strength of the correlation between γ' and various galaxy parameters are largely determined by the strength of the correlations with dark matter fraction (see Fig. 5).

5 ENSEMBLE MASS DENSITY SLOPE

In this section, we comment on a method to infer the average mass density slope of the dark matter within the effective radii of massive early-type galaxies. This method was recently used by Grillo (2012) to argue in favor of very steep dark matter density profiles, which is in apparent contradiction to our results (as well as those by Auger et al. 2010a).

The main observables are the total projected mass, $M_{tot}(R_{Ein})$, within the Einstein radius, R_{Ein} , obtained from strong gravitational lensing. For a given IMF one can calculate the total mass in stars, M_{SPS} , and the mass in stars within the Einstein radius, $M_{SPS}(< R_{Ein})$. Thus for each lens, assuming an IMF, one can calculate the dark matter surface density within the Einstein radius:

$$\Sigma_{DM}(R_{Ein}) = [M_{tot}(< R_{Ein}) - M_{SPS}(< R_{Ein})] / \pi R_{Ein}^2. \quad (3)$$

Since the Einstein radii are in general different for each lens system, one can determine the average dark matter density profile for an ensemble of gravitational lenses (see, e.g., Rusin & Kochanek 2005 for a similar strategy). However, the lenses have different masses and sizes, and therefore the ensemble average cannot be conducted in physical scales. A useful approach is to scale the size and density measurements with the intrinsic scales of the galaxies: the effective radii R_e , and effective surface densities $\Sigma_e \equiv M_{SPS}/R_e^2$. In this way, one can then define dimensionless sizes and dark matter densities via

$$\Lambda = R_{Ein}/R_e, \quad (4)$$

and

$$\Psi = \Sigma_{DM}(R_{Ein})/\Sigma_e(R_e). \quad (5)$$

Plotting Ψ versus Λ thus yields an ensemble density profile of the dark matter. The correlation can be described with a power law:

$$\Psi = \alpha \Lambda^\beta \quad (6)$$

to yield an effective de-projected dark matter density slope $\gamma'_{DM,g} = -\beta + 1$.

Applying this method to 39 massive early-type lenses from the SLACS survey, Grillo (2012) found $\beta = -1.04^{+0.26}_{-0.22}$ (corresponding to $\gamma'_{DM,g} = 2.04^{+0.22}_{-0.26}$) for a Chabrier IMF, and $\beta = -0.77^{+0.62}_{-0.37}$ (corresponding to $\gamma'_{DM,g} = 1.77^{+0.37}_{-0.62}$) for a Salpeter IMF. Since an uncontracted NFW halo will have $\beta \simeq -0.1$ ($\gamma'_{DM} \simeq 1.1$), this provides marginal evidence for halo contraction in response to galaxy formation (assuming the IMF is lighter than Salpeter), in contradiction to our results. However, as we discuss below, there are two issues that explain this apparent discrepancy.

The first issue is that the IMF is likely Salpeter or

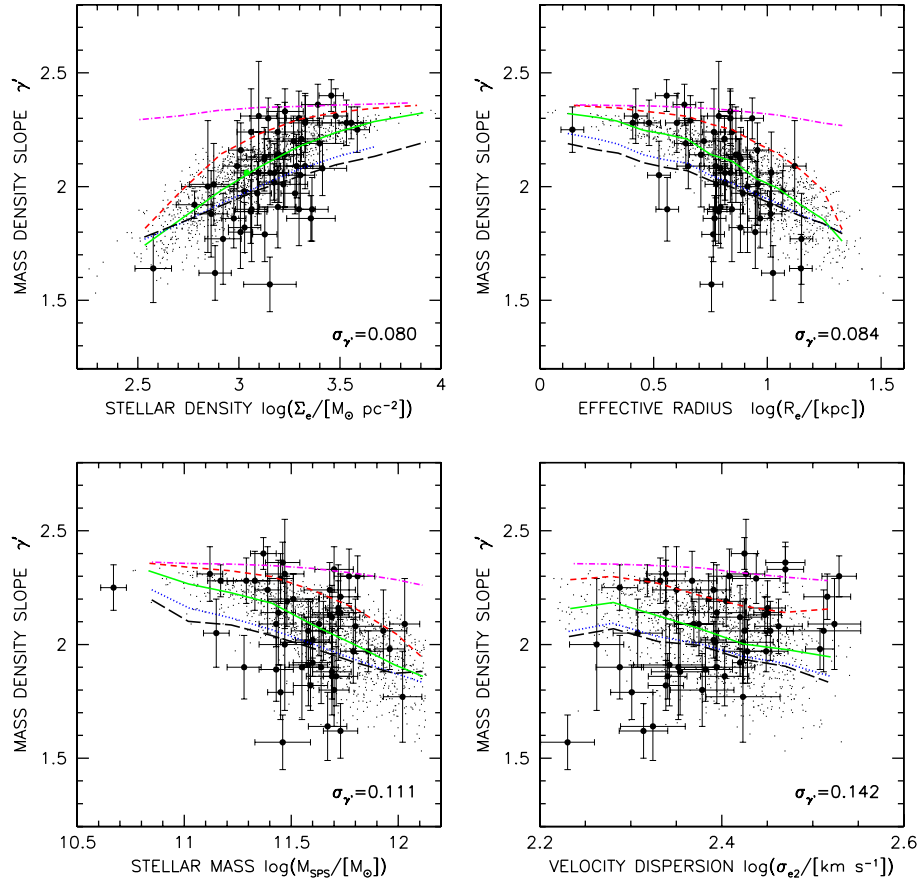


Figure 4. Correlations between mass density slope within the effective radius, γ' , and galaxy observables: stellar surface density (Σ_e , upper left), effective radius (R_e , upper right), stellar mass (M_{SPS} , lower left) and stellar velocity dispersion (σ_{e2} , lower right). The models are given by coloured lines: adiabatic contraction ($\nu = 1.0$, black long dashed); mild contraction ($\nu = 0.5$, blue dotted); no contraction ($\nu = 0.0$, green solid); halo expansion ($\nu = -0.5$, red short dashed). In addition, the points show individual galaxies for the no contraction model (which provides the best match to the observed mean and scatter of γ' – see Fig. 1). The scatter about the median relation for this model, $\sigma_{\gamma'}$, is given in the lower right corner of each panel. The tightest correlation in the models is between γ' and stellar density, while the weakest is with velocity dispersion. The data from SLACS (Auger et al. 2010b) are given by filled symbols with error bars. For both models and data the stellar masses and surface densities have been scaled to a Salpeter IMF. The trends seen in the no contraction model are also seen in the observations, providing further support for its validity.

heavier, which will obviously require shallower dark matter slopes. For example, Auger et al. (2010a), Dutton et al. (2013b), and Conroy & van Dokkum (2012) all favour IMFs Salpeter or heavier in the most massive galaxies. We note that for a Salpeter IMF or heavier our results are in agreement with Grillo’s.

The second issue is more subtle and has to do with an implicit assumption of the method used by Grillo (2012). Grillo assumes that the re-scaling of the dark matter densities and Einstein radii does not introduce spurious correlations. Specifically, in order for $\Psi(\Lambda)$ to be equivalent to $\Sigma_{\text{DM}}(R_{\text{Ein}})$ requires that $\Sigma_{\text{SPS}}/R_e^\beta$ is independent of R_{Ein} . Using SLACS data from Auger et al. (2010b), we find that this is not the case. Fitting a relation of the form $\Sigma_e/R_e^\beta \propto (R_{\text{Ein}})^\delta$ on a grid of β over the interval $[-2.5, 1]$, and then fitting a linear relation between δ and β we find that $\delta = -0.078 - 0.586\beta$. Thus, the true dark matter density slope is given by

$$\gamma'_{\text{DM}} \equiv \gamma'_{\text{DM,g}} - \delta = 0.664 + 0.414\gamma'_{\text{DM,g}}. \quad (7)$$

So a measured isothermal mass slope (i.e., $\gamma'_{\text{DM,g}} = 2$) implies a shallower true mass slope of $\gamma'_{\text{DM}} = 1.49$.

Correcting the results from Grillo (2012) using Eq. 7 yields $\gamma'_{\text{DM,g}} = 1.51^{+0.10}_{-0.11}$ for a Chabrier IMF, and $\gamma'_{\text{DM,g}} = 1.40^{+0.15}_{-0.26}$ for a Salpeter IMF. In the context of our models, this would favour weak contraction ($\nu \sim 0.5$), which is similar to that found in cosmological simulations by Abadi et al. (2010). Allowing for an IMF slightly heavier than Salpeter (as we favour) would increase the inferred β to be in even closer agreement with our results. In summary, we find that there is no conflict between the ensemble average dark matter density slope as derived by Grillo (2012) and our results based on the fundamental plane and total mass density slopes

6 DISCUSSION

We have shown that the observed distribution of mass density slopes can be reproduced, *precisely*, if galaxies with re-

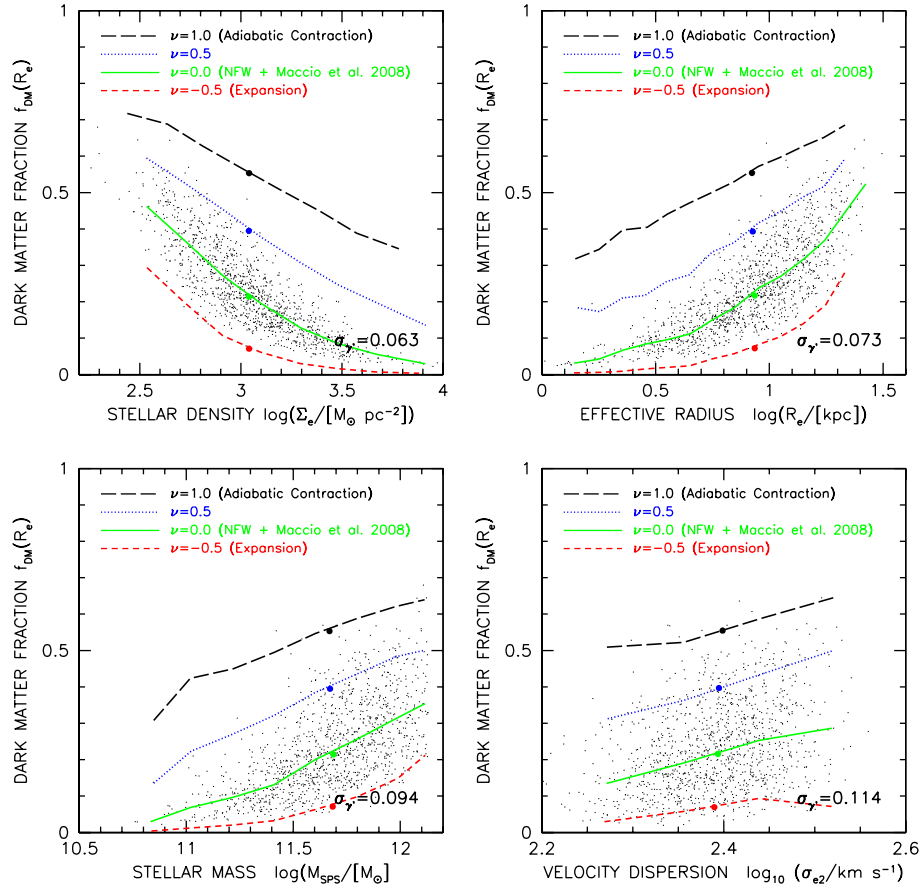


Figure 5. Correlations between dark matter fraction within the effective radius, $f_{\text{DM}}(R_e)$, and galaxy observables (as in Fig. 4) for our models. The scatter about the median relation for the no contraction model, σ_γ , is given in the lower-right corner of each panel. The size of the scatter in these relations is directly correlated with the size of the scatter in the equivalent relations in Fig. 4.

alistic sizes and concentrations are embedded in cosmologically motivated dark matter haloes. We note that a key requirement for our models to reproduce the observed γ' is that the concentration of the stars needs to be high enough so that $\gamma'_{\text{star}}(R_e) > 2$ — because Λ CDM haloes on their own never have such steep density profiles on such scales. For example, galaxies with exponential surface density profiles (i.e., characteristic of galaxy discs) would be unable to result in $\gamma'(R_e) \sim 2$.

Our model assumes that the scatter in galaxy sizes at fixed stellar mass is uncorrelated with the structure of the dark matter halo. This assumption was made for simplicity (and remarkably it seems to work), but it should be tested using galaxy formation models. For example, for spiral galaxies we *do* expect correlations between the scatter in galaxy sizes with scatter in halo concentrations and galaxy formation efficiencies (see Fig.7 in Dutton et al. 2007). It remains to be seen whether such correlations exist for spheroid dominated galaxies.

Our results favour unmodified cosmologically motivated (Navarro et al. 1997; Macciò et al. 2008) dark matter haloes. This is somewhat surprising, since there are many processes that should modify the dark halo structure (e.g., gas accretion, gas outflows, minor and major mergers). One possibility is that these various processes are occurring stochasti-

cally, and cancel each other out on average. Alternatively, we might expect that gas accretion dominates at early times, followed by gas outflows, then dry mergers. Under this scenario, we would expect the halo to initially contract, and then to slowly undo this contraction over time. Thus a measurement of the evolution of the halo response would be able to distinguish between these formation scenarios for massive elliptical galaxies. This should be possible with the current generation of galaxy scale lenses extending to higher redshifts than SLACS (Sonnenfeld et al. 2013).

Recently, Chae et al. (2014) have performed a complementary analysis of the mass density profiles of early-type galaxies in the SDSS. These authors find an average mass density slope of $\langle \gamma_e \rangle = 2.15 \pm 0.04$, where individual γ_e are obtained from power-law fits to the total density profiles between 0.1 and 1.0 effective radii. These results appear steeper than our uncontracted halo models, as well as the slopes inferred from strong lensing studies at low redshift (e.g., Auger et al. 2010b). However, since Chae et al. (2013) adopt a different definition for the mass density slope, a detailed comparison between our respective results is non-trivial. Ideally, comparisons with mass density slopes derived from strong lensing studies would employ the same method on model galaxies as is applied to the lenses.

7 CONCLUSIONS

In the past few years observations have shown that massive early-type galaxies have close to isothermal density profiles within one effective radius (Koopmans et al. 2009; Auger et al. 2010b). We use Λ CDM-based mass models constructed to reproduce a number of the observed scaling relations of early-type galaxies (including the Faber-Jackson relation) to address two questions: (1) For models with the correct distribution of baryons, do the properties of Λ CDM haloes result in models that reproduce the observed properties of γ' ? (2) Do the observed properties of γ' help to distinguish between models with different stellar initial mass functions? We summarize our results as follows.

- The median values of the mass density slopes of all our models are roughly isothermal: $1.8 \lesssim \gamma' \lesssim 2.4$. The observed mean value of $\langle \gamma' \rangle = 2.08 \pm 0.03$ is best reproduced by a model with uncontracted NFW haloes and stellar masses $\simeq 0.27$ dex higher than that obtained assuming a Chabrier (2003) IMF (Fig. 1).
- The scatter in γ' in our models with dark matter haloes is small $0.10 \lesssim \sigma_{\gamma'} \lesssim 0.17$. The observed (intrinsic) scatter of $\sigma_{\gamma'} = 0.16 \pm 0.02$ is best reproduced by our model with uncontracted dark matter haloes (Fig. 1).
- In observations the mass density slope correlates with stellar surface density and effective radius, with higher γ' in higher density and smaller galaxies. As with other properties of γ' this correlation is best reproduced by our model with uncontracted NFW haloes (Fig. 4).
- In the models the tightness of the correlations involving γ' are largely determined by the tightness of the corresponding correlations involving (spherical) dark matter fraction within the effective radius (Fig. 5).

In conclusion, our study shows that the many of the observed properties – including the bulge-halo conspiracy and other classic scaling relations like the Faber Jackson and size mass relation – of massive early-type galaxies can be *precisely* reproduced by Λ CDM models under two conditions: (i) the IMF is not universal; (ii) mechanisms, such as feedback from active galactic nuclei or dynamical friction, effectively counterbalance on average the contraction of the halo expected as a result of baryonic cooling. We emphasize that no correlations between the scatter in galaxy and dark halo parameters (or equivalently, no fine-tuning between the baryons and dark matter) is needed in order for our models to reproduce the observed small scatter in total mass density profiles. Although our models are clearly an oversimplified description of reality, they demonstrate that self-consistent Λ CDM-inspired models can be found. This gives hope that the recent improvements in numerical simulations including baryonic physics could soon lead to realistic models for the formation of massive type galaxies in quantitative agreement with the tight constraints provided by observations. In turn, this might help explain what is the relative contribution of the different processes that contribute to produce the effective profiles that we observe. Our work also provides further evidence against a universal IMF for galaxies. In agreement with earlier studies (Auger et al. 2010a; van Dokkum & Conroy 2010; Spiniello et al. 2011; Sonnenfeld et al. 2012; Conroy & van Dokkum 2012; Smith et al. 2012; Spiniello et al. 2012; Cappellari et al. 2013; Dutton et al. .

2013a,b), we find that a “heavy” Salpeter-like IMF is preferred for massive galaxies over the light Chabrier-like IMFs usually preferred for Milky Way-type galaxies. The origin of this non-universality is still hotly debated. However, the fact that the only quantity that seems to correlate with the mass structure of massive early-type galaxies is the central surface density could be a clue that the density of stars (and therefore possibly gas at the epoch of peak star formation) is an important ingredient of shaping the final stellar initial mass function (Hopkins 2013).

ACKNOWLEDGEMENTS

We thank our friends and colleagues of the SLACS and SWELLS collaborations for numerous stimulating discussions about these topics over the years. We also thank the participants of Lorentz Workshop “Is the stellar IMF universal?”, in particular the organizers (Leon Koopmans, Scott Trager, Romeel Davé, Patrick Hennebelle, Chris McKee, Michael Meyer, Stella Offner) for illuminating presentations and conversations. We are also grateful to the staff at Lorentz Center in particular Ms Gerda Filippo for her making the workshop a wonderful experience.

AAD acknowledges financial support from the National Science Foundation Science and Technology Center CfAO, managed by UC Santa Cruz under cooperative agreement no. AST-9876783. TT acknowledges support from the NSF through CAREER award NSF-0642621, and from the Packard Foundation through a Packard Research Fellowship. This research was partially supported by NASA through Hubble Space Telescope programs GO-10587, GO-10886, GO-10174, 10494, 10798, 11202.

REFERENCES

- Abadi, M. G., Navarro, J. F., Fardal, M., Babul, A., & Steinmetz, M. 2010, MNRAS, 407, 435
- Abazajian, K. N., et al. 2009, ApJS, 182, 543
- Allen, S. W., Rapetti, D. A., Schmidt, R. W., et al. 2008, MNRAS, 383, 879
- Auger, M. W., Treu, T., Bolton, A. S., et al. 2009, ApJ, 705, 1099
- Auger, M. W., Treu, T., Gavazzi, R., Bolton, A. S., Koopmans, L. V. E., & Marshall, P. J. 2010a, ApJL, 721, L163
- Auger, M. W., Treu, T., Bolton, A. S., Gavazzi, R., Koopmans, L. V. E., Marshall, P. J., Moustakas, L. A., & Burles, S. 2010b, ApJ, 724, 511
- Bastian, N., Covey, K. R., & Meyer, M. R. 2010, ARA&A, 48, 339
- Bell, E. F., & de Jong, R. S. 2001, ApJ, 550, 212
- Bell, E. F., McIntosh, D. H., Katz, N., & Weinberg, M. D. 2003, ApJS, 149, 289
- Bertin, G., Bertola, F., Buson, L. M., et al. 1994, A&A, 292, 381
- Blumenthal, G. R., Faber, S. M., Flores, R., & Primack, J. R., 1986, ApJ, 301, 27
- Bolton, A. S., Burles, S., Koopmans, L. V. E., Treu, T., & Moustakas, L. A. 2006, ApJ, 638, 703
- Bolton, A. S., Burles, S., Koopmans, L. V. E., Treu, T.,

- Gavazzi, R., Moustakas, L. A., Wayth, R., & Schlegel, D. J. 2008, *ApJ*, 682, 964
- Bolton, A. S., Brownstein, J. R., Kochanek, C. S., et al. 2012, *ApJ*, 757, 82
- Cappellari, M., et al. 2006, *MNRAS*, 366, 1126
- Cappellari, M., McDermid, R. M., Alatalo, K., et al. 2013, *MNRAS*, 432, 1862
- Chabrier, G. 2003, *PASP*, 115, 763
- Chae, K.-H., Bernardi, M., & Kravtsov, A. V. 2014, *MNRAS*, 437, 3670
- Ciotti, L., Lanzoni, B., & Renzini, A. 1996, *MNRAS*, 282, 1
- Conroy, C., & van Dokkum, P. G. 2012, *ApJ*, 760, 71
- Dobke, B. M., & King, L. J. 2006, *A&A*, 460, 647
- Dressler A., Faber S. M., Burstein D., Davies R. L., Lynden-Bell D., Terlevich R. J., Wegner G., 1987, *ApJ*, 313, L37
- Djorgovski S., Davis M., 1987, *ApJ*, 313, 59
- Dubois, Y., Gavazzi, R., Peirani, S., & Silk, J. 2013, *MNRAS*, 433, 3297
- Duffy, A. R., Schaye, J., Kay, S. T., Dalla Vecchia, C., Battye, R. A., & Booth, C. M. 2010, *MNRAS*, 405, 2161
- Dutton, A. A., van den Bosch, F. C., Dekel, A., & Courteau, S. 2007, *ApJ*, 654, 27
- Dutton, A. A., Conroy, C., van den Bosch, F. C., Prada, F., & More, S. 2010, *MNRAS*, 407, 2
- Dutton, A. A., Conroy, C., van den Bosch, F. C., et al. 2011, *MNRAS*, 416, 322
- Dutton, A. A., Macciò, A. V., Mendel, J. T., & Simard, L. 2013b, *MNRAS*, 432, 2496
- Dutton, A. A., Treu, T., Brewer, B. J., et al. 2013a, *MNRAS*, 428, 3183
- Einasto, J. 1965, *Trudy Astrofizicheskogo Instituta Alma-Ata*, 5, 87
- El-Zant, A. A., Shlosman, I., & Hoffman, Y. 2001, *ApJ*, 560, 636
- Faber, S. M., & Jackson, R. E. 1976, *ApJ*, 204, 668
- Franx, M., van Gorkom, J. H., & de Zeeuw, T. 1994, *ApJ*, 436, 642
- Gavazzi, R., Treu, T., Rhodes, J. D., et al. 2007, *ApJ*, 667, 176
- Gnedin, O. Y., Kravtsov, A. V., Klypin, A. A., & Nagai, D. 2004, *ApJ*, 616, 16
- Governato, F., et al. 2010, *Nature*, 463, 203
- Grillo, C. 2012, *ApJL*, 747, L15
- Hopkins, P. F. 2013, *MNRAS*, 433, 170
- Humphrey, P. J., & Buote, D. A. 2010, *MNRAS*, 403, 2143
- Jiang, G., & Kochanek, C. S. 2007, *ApJ*, 671, 1568
- Jardel, J. R., & Sellwood, J. A. 2009, *ApJ*, 691, 1300
- Johansson, P. H., Naab, T., & Ostriker, J. P. 2009, *ApJL*, 697, L38
- Johansson, P. H., Naab, T., & Ostriker, J. P. 2012, *ApJ*, 754, 115
- Keeton, C. R. 2001, *ApJ*, 561, 46
- Koopmans, L. V. E., Treu, T., Bolton, A. S., Burles, S., & Moustakas, L. A. 2006, *ApJ*, 649, 599
- Koopmans, L. V. E., Bolton, A., Treu, T., et al. 2009, *ApJL*, 703, L51
- Macciò, A. V., Dutton, A. A., & van den Bosch, F. C. 2008, *MNRAS*, 391, 1940
- Macciò, A. V., Stinson, G., Brook, C. B., et al. 2012, *ApJL*, 744, L9
- Mandelbaum, R., Seljak, U., Kauffmann, G., Hirata, C. M., & Brinkmann, J. 2006, *MNRAS*, 368, 715
- Merritt, D., Navarro, J. F., Ludlow, A., & Jenkins, A. 2005, *ApJL*, 624, L85
- Merritt, D., Graham, A. W., Moore, B., Diemand, J., & Terzić, B. 2006, *AJ*, 132, 2685
- More, S., van den Bosch, F. C., Cacciato, M., Skibba, R., Mo, H. J., & Yang, X. 2011, *MNRAS*, 410, 210
- Naab T., Johansson P. H., Ostriker J. P., Efstathiou G., 2007, *ApJ*, 658, 710
- Navarro, J. F., Frenk, C. S., & White, S. D. M. 1997, *ApJ*, 490, 493
- Navarro, J. F., Hayashi, E., Power, C., et al. 2004, *MNRAS*, 349, 1039
- Navarro, J. F., Ludlow, A., Springel, V., et al. 2010, *MNRAS*, 402, 21
- Newman A. B., Treu T., Ellis R. S., Sand D. J., Nipoti C., Richard J., Jullo E., 2013a, *ApJ*, 765, 24
- Newman A. B., Treu T., Ellis R. S., Sand D. J., 2013b, *ApJ*, 765, 25
- Nipoti C., Treu T., Ciotti L., Stiavelli M., 2004, *MNRAS*, 355, 1119
- Nipoti C., Treu T., Bolton A. S., 2008, *MNRAS*, 390, 349
- Nipoti C., Treu T., Leauthaud A., Bundy K., Newman A. B., Auger M. W., 2012, *MNRAS*, 422, 1714
- Pontzen, A., & Governato, F. 2012, *MNRAS*, 421, 3464
- Read, J. I., & Gilmore, G. 2005, *MNRAS*, 356, 107
- Reed, D. S., Koushiappas, S. M., & Gao, L. 2011, *MNRAS*, 415, 3177
- Remus, R.-S., Burkert, A., Dolag, K., et al. 2013, *ApJ*, 766, 71
- Ruff, A. J., Gavazzi, R., Marshall, P. J., et al. 2011, *ApJ*, 727, 96
- Rusin, D., & Kochanek, C. S. 2005, *ApJ*, 623, 666
- Salpeter, E. E. 1955, *ApJ*, 121, 161
- Schulz, A. E., Mandelbaum, R., & Padmanabhan, N. 2010, *MNRAS*, 408, 1463
- Simard, L., Mendel, J. T., Patton, D. R., Ellison, S. L., & McConnell, A. W. 2011, *ApJS*, 196, 11
- Smith, R. J., Lucey, J. R., & Carter, D. 2012, *MNRAS*, 426, 2994
- Sonnenfeld, A., Treu, T., Gavazzi, R., et al. 2012, *ApJ*, 752, 163
- Sonnenfeld, A., Treu, T., Gavazzi, R., et al. 2013, *ApJ*, 777, 98
- Spiniello, C., Koopmans, L. V. E., Trager, S. C., Czoske, O., & Treu, T. 2011, *MNRAS*, 417, 3000
- Spiniello, C., Trager, S. C., Koopmans, L. V. E., & Chen, Y. P. 2012, *ApJL*, 753, L32
- Stadel, J., Potter, D., Moore, B., et al. 2009, *MNRAS*, 398, L21
- Teyssier, R., Moore, B., Martizzi, D., Dubois, Y., & Mayer, L. 2011, *MNRAS*, 414, 195
- Tortora, C., La Barbera, F., Napolitano, N. R., de Carvalho, R. R., & Romanowsky, A. J. 2012, *MNRAS*, 425, 577
- Treu, T., & Koopmans, L. V. E. 2004, *ApJ*, 611, 739
- Treu, T., Auger, M. W., Koopmans, L. V. E., Gavazzi, R., Marshall, P. J., & Bolton, A. S. 2010, *ApJ*, 709, 1195
- van Dokkum, P. G., & Conroy, C. 2010, *Nature*, 468, 940
- York, D. G., et al. 2000, *AJ*, 120, 1579